Available online at www.sciencedirect.com
SCIENCE DIRECT®
Thin Solid Films 453–454 (2004) 584–588
thin solid films
www.elsevier.com/locate/tsf

Time resolved study of the laser ablation induced shockwave

M. Hauer[a], D.J. Funk[b], T. Lippert[a,*], A. Wokaun[a]

[a]*General Energy Research, Paul Scherrer Institut, 5232 Villigen PSI, Switzerland*
[b]*DX-2, MS C920, Los Alamos National Laboratory, Los Alamos, NM 87545, USA*

Abstract

Laser ablation is used in laser plasma thrusters (LPT), in which the created plasma provides the thrust that is used to stabilize the trajectory of satellites in space. To allow the use of IR laser diodes, an IR absorber has to be added to the polymer. As a measure of the energy released during ablation of such polymers, the shockwave velocity in air is measured with shadowgraphy. The measured shockwave velocities of a cross-linked glyzidyl azide polymer (GAP) incorporating carbon particles (as broad range absorber), reveal that the shockwave velocity decreases with the increasing irradiation wavelength (193–1064 nm) for a given fluence. In addition, the shadowgraph images reveal that for irradiation with shorter wavelengths, the amount of solid fragments decreases and more gaseous products are released. Comparing the shockwave propagation of GAP and a triazene polymer reveals that both polymers exhibit similar shockwave velocities at UV irradiation wavelength, whereas with 1064 nm irradiation, the shockwaves generated using GAP propagate faster. These results are probably due to the change of the absorption site, the mechanism of ablation, and the different decomposition enthalpies.

Keywords: Laser ablation; Shockwave; Polymer; Shadowgraphy

1. Introduction

During the 20 years since the first reports on laser ablation of polymers a wide variety of potential commercial applications have been discussed [1]. In most of the applications, the shockwave and particles generated during the ablation process influence the performance and quality of these techniques. In many lithographic applications, the re-deposition of the ejected particles as debris is a major problem [1–3]. In other applications, the laser plasma is used to generate a certain thrust (laser plasma thrusters [4,5]) or to transfer material from a target layer to a receiving layer (laser material transfer [6–8]). Understanding the magnitude of the energy released and how the material is ejected during the ablation process can provide insight as to how to improve these applications.

Time resolved ns-shadowgraphy can be applied to observe the released fragments and the shockwave after laser irradiation [9–13]. The measured propagation velocity can be used as a measure of the energy released during the ablation process and, therefore, for the performance of these materials in LPT's. In these devices, the plasma provides the thrust that is used to stabilize the trajectory of satellites in space. It has been shown that an energetic polymer (glyzidyl azide polymer (GAP)) produces a ratio between thrust and laser energy that is higher than for other polymers [4,5]. Since these devices use IR laser diodes as light sources, carbon particles, as broadband absorber, were added to the GAP prior to cross-linking. To measure the influence of the absorption site (absorber or polymer) different irradiation wavelengths ranging from UV (193 nm) to the near IR (1064 nm) were used.

Complementary information was obtained by comparing the shockwave generated with GAP to a triazene polymer (TP). This polymer was especially designed for 308-nm irradiation, exhibits superior laser ablation properties, and decomposes exothermally.

2. Experimental

The preparation of GAP was done according to a procedure previously described [14]. Carbon particles (1 wt.% of the polymer) were added before cross-linking of the polymer to increase the IR absorption coefficient ($\alpha_{\mathrm{lin,1064\ nm}} = 400\ \mathrm{cm}^{-1}$). The TP was pre-

*Corresponding author. Tel.: +41-56-310-4076; fax: +41-56-310-4412.
E-mail address: thomas.lippert@psi.ch (T. Lippert).

0040-6090/04/$ - see front matter © 2003 Elsevier B.V. All rights reserved.
doi:10.1016/j.tsf.2003.11.139

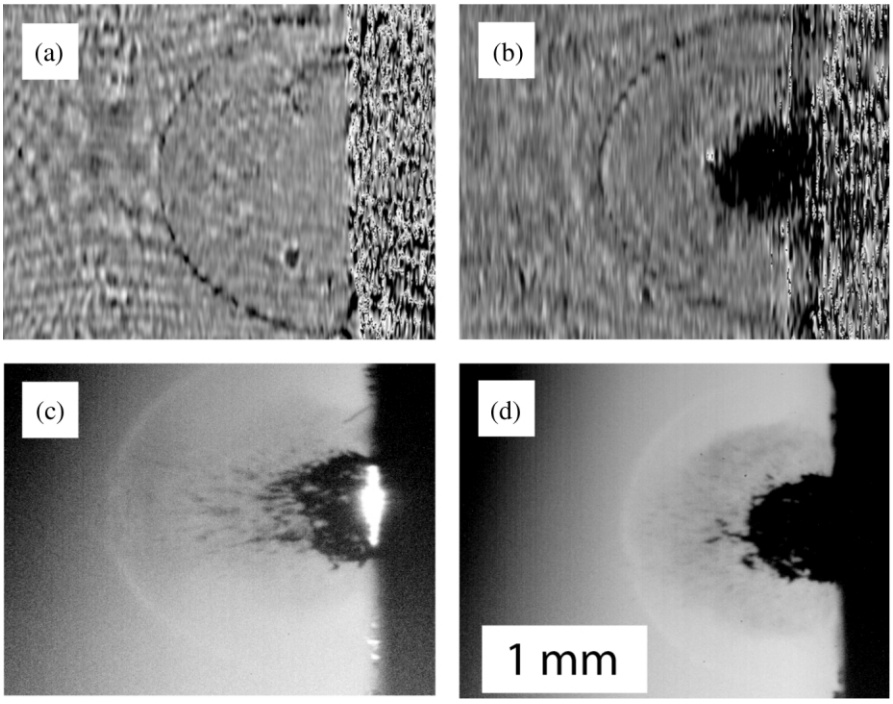

Fig. 1. Shadowgraphy images after laser irradiation: (a) and (b) were taken with interference shadowgraphy, (c) and (d) were taken with conventional shadowgraphy. (a) 193 nm with 1.6 mJ pulse^{-1}, delay 0.9 μs; (b) 308 nm, with 2.6 mJ pulse^{-1}, delay 1 μs; (c) 532 nm, with 11 mJ pulse^{-1}, delay 1 μs; (d) 1064 nm, with 11.2 mJ pulse^{-1}, delay 1 μs.

pared according to a procedure previously published [15]. A solution of 10 wt.% of the polymer in chlorobenzene was solvent cast onto a cover glass and dried. For the measurements at 1064 nm irradiation, carbon particles were added to the TP solution (0.75 wt.% of the polymer), prior to casting. The IR absorption coefficient of TP was similar to ($\alpha_{\mathrm{lin,1064\ nm}} = 420\ \mathrm{cm}^{-1}$) the absorption coefficient of GAP. The absorption coefficients of the polymers at 193 nm (GAP + 1% C, $\alpha_{\mathrm{lin,193\ nm}} = 44\,000\ \mathrm{cm}^{-1}$; TP, $\alpha_{\mathrm{lin,193\ nm}} = 116\,000\ \mathrm{cm}^{-1}$) were not measurably affected by the addition of the carbon particles. Therefore, the ablation behavior after 193 nm irradiation should not be affected by the carbon particles.

The shadowgraphy measurements were performed in a pump-probe setup. For irradiations with the UV wavelengths, a XeCl (308 nm, Compex 205 from Lambda Physik, FWHM 30 ns) or an ArF (193 nm, LPX 301i from Lambda Physik, FWHM 25 ns) excimer laser was used (spot diameter approx. 530 ± 50 μm). The probe laser (2nd harmonic of an Brillant Bw Nd:YAG laser from Quantel, FWHM of 6 ns) was used in a Mach-Zehnder interferometer. One beam of the interferometer passes parallel to surface of the polymer, through the ablation plume, while the other beam is unaffected by the ablation process. Both beams are recombined interferometrially in a second beamsplitter where the fringe pattern, which is recorded with a digital camera, is created. The compressed (i.e. ablation products and air) gases in the shockwave of the ablation have a higher optical density than the ambient atmosphere and thereby cause a fringe shift (phase displacement). A detailed description of the experimental setup and the evaluation of the fringe shift can be found in [12]. The time delay between both lasers was controlled with a generator (DG 535 from SRS).

For measurements at 532 and 1064 nm a conventional shadowgraphy setup was used. The second harmonic and fundamental of the Nd:YAG laser were used as a pump laser (spot diameter approx. 480 ± 15 μm). The beam profile of this laser was super-Gaussian with some hotspots. The ejected plume and shockwave were illuminated by the fluorescence from a methanol Rhodamin solution that was excited by the XeCl excimer laser. The resulting image was recorded by a digital camera, the axis of which was oriented parallel to the surface of the polymer.

3. Results and discussion

Fig. 1 shows the shockwave and the particles, which are generated during the laser ablation process of GAP. The first two images (a and b) are amplitude images obtained from interference shadowgraphy and show transmission through the ablation plume. The last two images (c and d) are obtained from classical shadow-

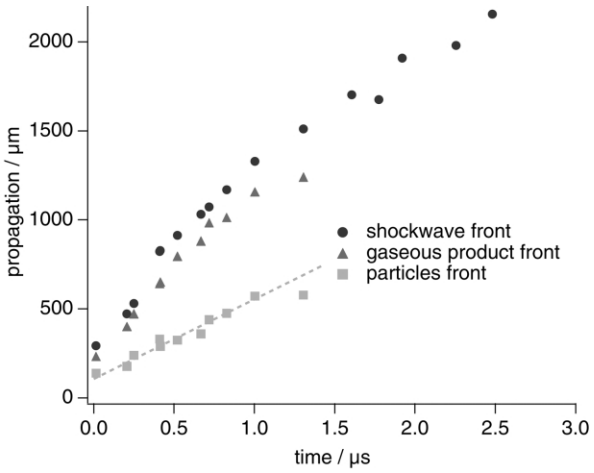

Fig. 2. Shockwave and particles expansion of GAP after 1064 nm with 11.2 mJ pulse^{-1}.

graphy. With 193 nm irradiation (Fig. 1a) only the shockwave is visible as a dark ring. With 308 nm irradiation, in addition to the shockwave, a darkening is observed that we attribute to the attenuation of the probe laser beam. A similar behavior is found with the 532 nm irradiation, where we observe a shockwave, followed by a dark center, that breaks into large fragments at late times (not shown). Upon irradiation with 1064 nm, the shockwave and two different product phases can be distinguished: a slightly darkened area behind the shockwave and a very dark center. The slightly darkened area is possibly due to small fragments. The center seems to consist of larger fragments, which later separate from each other (not shown).

With 193 nm irradiation the GAP is absorbing the laser light, whereas at wavelengths above 235 nm the laser energy is absorbed by the carbon particles. This results in much lower absorption coefficients (i.e. GAP: $\alpha_{\mathrm{lin,193\ nm}} = 44000\ \mathrm{cm}^{-1}$ vs. $\alpha_{\mathrm{lin,1064\ nm}} = 400\ \mathrm{cm}^{-1}$) and much higher ablation thresholds (GAP and TP: $F_{\mathrm{th,193\ nm}} \approx 0.02\ \mathrm{J\ cm}^{-2}$ vs. $F_{\mathrm{th,1064\ nm}} \approx 1.6\ \mathrm{J\ cm}^{-2}$, which corresponds to ablation threshold energies of approx. $E_{\mathrm{Th,193}} \approx 50\ \mu\mathrm{J}$ vs. $E_{\mathrm{Th,1064}} \approx 2.8\ \mathrm{mJ}$) at longer wavelengths. At 193 nm, the laser light is able to break the bonds within the polymer resulting in smaller fragments, which are not observed in the amplitude image. With longer wavelengths, the carbon particles absorb the laser energy and will cause a temperature increase leading to thermal decomposition of the polymer.

For irradiation at longer wavelengths, the energy is absorbed by the carbon particles. Therefore, the energy is, on a molecular level, not homogeneously absorbed, resulting in the formation of hotspots. These can cause an inhomogeneous decomposition of the polymer resulting in the ejection of more solid or liquid particles, which can be seen as a darkening in the shadowgraphy images.

The measured expansion of these particles (those of Fig. 1d) and the shockwave after 1064 nm irradiation of GAP are shown in Fig. 2. The front of small fragments follows the expansion curve of the shockwave. The front of larger fragments is expanding linearly with a velocity of 450 m s^{-1} and is not affected by the shockwave propagation. The larger fragments have, compared to the mass, a lower air drag than the smaller particles, and will de-accelerate much slower resulting in an almost linear propagation.

3.1. Wavelength dependence

Fig. 3 is a plot of the propagation of the shockwave front, using different irradiation wavelengths with similar irradiation energies. The shockwave velocity is increasing with the decrease of the irradiation wavelength. This indicates that, at these laser pulse energies, the created pressures and the amount of gaseous products increase with the decreasing wavelength (E_{plume} increases). As the irradiation wavelength decreases the photon energy and the density of absorption sites are increasing (α_{lin} increases). The higher photon energy and larger number of absorption sites result in more bond breaking and therefore in the larger amount of small gaseous products.

The penetration depth of the laser light increases with the increasing wavelength so that larger volumes are heated to a lower temperature. This will lead to a less efficient decomposition of the polymer at the longer irradiation wavelength. The loss of decomposition efficiency seems much more important than the gain due to the additionally ablated volume.

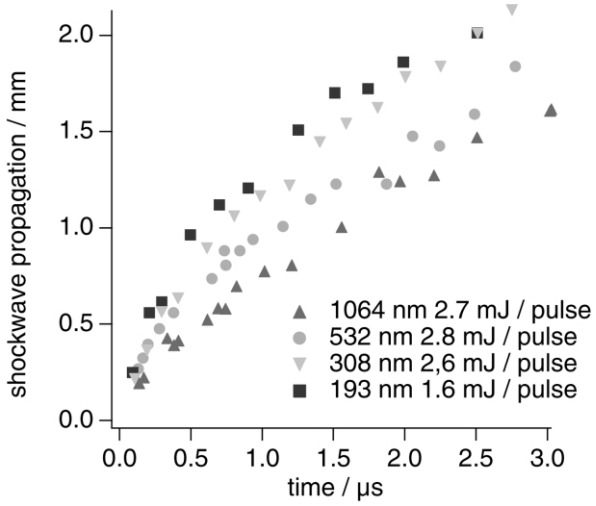

Fig. 3. Shockwave propagation of GAP with time as a function of the irradiation wavelength.

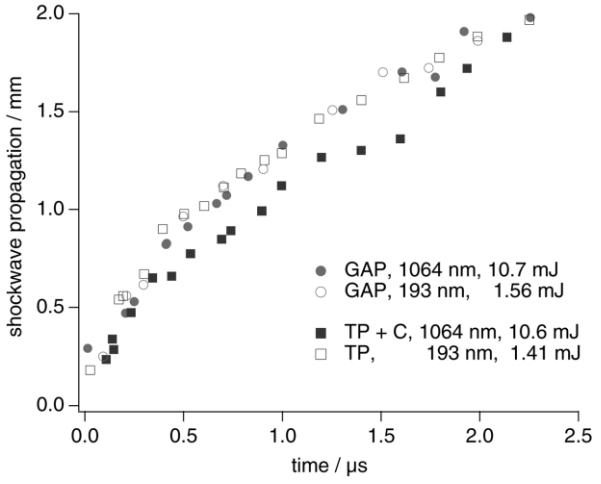

Fig. 4. Shockwave propagation of TP and GAP after 193 and 1064 nm irradiation. (The carbon particles do not affect the absorption at 193 nm and should therefore not influence the ablation behavior.)

This is confirmed by a model, describing the planar expansion of a shockwave [9,16], which concludes that the shockwave velocity increases with a decrease in the irradiated volume. As the penetration depth decreases with the wavelength, the shockwave should propagate faster for the same laser energy and spot size.

Fig. 1 shows that the amount of solid or liquid particles increases with the irradiation wavelength. The kinetic energy of these ejected particles (shown in Fig. 2 and described above) has also been provided by the laser energy or the decomposition enthalpy of the polymer and thereby reduces the energy available for the shockwave.

3.2. Material dependence for UV and IR wavelengths

Fig. 4 plots the shockwave propagation of TP and GAP after irradiation with 193 and 1064 nm. The velocity of the shockwave is similar for both polymers after 193 nm irradiation, whereas after 1064 nm irradiation, the shockwave propagation of GAP is faster than the shockwave propagation of TP (which was doped with carbon for the 1064 nm irradiation).

With 193 nm irradiation, the thresholds and the ablation rates of both polymers are of the same magnitude, so that comparable amounts of gaseous products are released (no particles were visible in the ejected plume). The resulting shockwave velocities are also similar. (The similarity between the shockwave velocity of GAP for 1064 and 193 nm irradiation is a coincidence and due to the very different laser energies.)

For 1064 nm higher ablation rates are observed for GAP compared to TP (for both polymers $E_{\mathrm{Laser}}/E_{\mathrm{Th}} \approx 3.8$). The above-mentioned model suggests that the shockwave velocity should, if the same energy is released, decrease with the ablation depth. The opposite behavior is found for 1064 nm irradiation ($d_{\mathrm{TP}} = 22$ μm vs. $d_{\mathrm{GAP}} = 42$ μm). This can be explained by the decomposition enthalpies of both polymers. The thermal decomposition enthalpy of GAP (2050 J g^{-1}) is approximately 3 times higher than the decomposition enthalpy of TP (697 J g^{-1}). This increases the amount of energy (assuming complete polymer decomposition: GAP: $E_{\mathrm{decomp}} \approx 20$ mJ vs. TP: $E_{\mathrm{decomp}} \approx 3.3$ mJ) released during the ablation process and increases thereby the propagation velocity of the shockwave released by GAP. In contrast, as the ablated volumes for 193 nm irradiations (for both polymers $E_{\mathrm{Laser}}/E_{\mathrm{Th}} \approx 30$) are much smaller ($d_{\mathrm{GAP}} = 0.5$ μm, $d_{\mathrm{TP}} = 0.2$ μm), the energy gain due to the decomposition enthalpy is not relevant in comparison to the laser energy.

4. Conclusion

The shadowgraphy images show that the amounts of non-gaseous particles increase with the wavelength. This behavior could be explained with the change of absorption site, the resulting changes in the ablation threshold and depth, and the inhomogeneities of absorption in the material due to the introduction of absorber particles.

It was found that the larger fragments propagate linearly and are independent of the propagation of the shockwave, while the smaller fragments seem to follow the propagation of the shockwave.

The shockwave velocity and thereby the energy of the explosion released in the plume decreases with increasing wavelength. This behavior might be attributed to the increase of the penetration depth with the wavelength. At longer wavelengths, a larger volume is heated to lower temperatures resulting in a less efficient decomposition of the polymer. A comparison with a model describing the shockwave suggests that the increase in ablation rate should additionally decrease the shockwave velocity.

The comparison of GAP with TP showed a pronounced difference in the shockwave velocity after 1064 nm irradiation while no difference was found after 193 nm irradiation. The difference at 1064 nm might be attributed to the differences in the decomposition enthalpies of both polymers.

Acknowledgments

The authors would like to thank Nitro Chemie Wimnis for supplying chemicals. This material is based upon the work supported by the European Office of Aerospace Research and Development, Air Force Office of Scientific Research, Air Force Laboratory, under contract F61775-01-WE057 and the Swiss National Science Foundation.

References

[1] P.E. Dyer, Appl. Phys. A 77 (2003) 167–173.
[2] P.E. Dyer, S.D. Jenkins, J. Sidhu, Appl. Phys. Lett. 49 (1986) 453.
[3] T. Lippert, J.T. Dickinson, Chem. Rev. 103 (2) (2003) 453–485.
[4] C.R. Phipps, J.R. Luke, G.G. McDuff, T. Lippert, SPIE 4760 (2002) 833–842.
[5] J.R. Luke, C.R. Phipps, G. Glen McDuff, SPIE 4760 (2002) 843–851.
[6] H. Fukumura, J. Photochem. Photobiol. A 106 (1997) 3–8.
[7] H. Fukumura, Y. Kohji, H. Masuhara, Appl. Surf. Sci. 96–98 (1996) 569–571.
[8] D.M. Karnakis, T. Lippert, N. Ichinose, S. Kasanishi, H. Fukumura, Appl. Surf. Sci. 127–129 (1998) 781–786.
[9] L.S. Bennett, T. Lippert, H. Furutani, H. Fukumura, H. Masuhara, Appl. Phys. A 63 (1996) 327–332.
[10] R. Srinivasan, B. Braren, K.G. Casey, M. Yeh, Appl. Phys. Lett. 55 (1989) 2790–2791.
[11] P.E. Dyer, D.M. Karnakis, P.H. Key, J.P. Tait, Appl. Surf. Sci. 96–98 (1996) 596–600.
[12] M. Hauer, D.J. Funk, T. Lippert, A. Wokaun, SPIE Proc. 4760 (2002) 259.
[13] Y.B. Eliahu, Y. Haas, J. Phys. Chem. 99 (1995) 6010–6018.
[14] C-J. Tang, Y. Lee, T.A. Litzinger, Combust. Flame 117 (1999) 244–256.
[15] J. Stebani, O. Nuyken, T. Lippert, A. Wokaun, Makromol. Chem. Rapid Commun. 206 (1993) 2943.
[16] D.A. Freiwald, J. Appl. Phys. 43 (1972) 2224–2226.